Isobaric yield ratio difference and neutron density difference in calcium isotopes

C. W. Ma (马春旺),[1,*] J. Yu (余姣),[1] X. M. Bai (白晓曼),[1] Y. L. Zhang (张艳丽),[1]
H. L. Wei (魏慧玲),[1] and S. S. Wang (王闪闪)[1,2]
[1]*Institute of Particle and Nuclear Physics, Henan Normal University, Xinxiang 453007, China*
[2]*Shanghai Institute of Applied Physics, Chinese Academy of Sciences, Shanghai 201800, China*
(Received 13 February 2014; revised manuscript received 9 April 2014; published 12 May 2014)

The isobaric yield ratio difference between two reactions is found to equal $\Delta\mu_{21}/T$, which denotes the ratio of the difference between the neutron and proton chemical potentials to the temperature. A series of projectile fragmentation reactions induced by calcium isotopes are calculated using a modified statistical abrasion-ablation model, assuming the neutron density distribution to be the Fermi type. The $\Delta\mu_{21}/T$ from the prefragments are found to be sensitive to the difference between the neutron density distributions of projectiles, while $\Delta\mu_{21}/T$ from the final fragments are very similar for the reactions and insensitive to the difference between the neutron density distributions of projectiles. The $\Delta\mu_{21}/T$ from the prefragments and final fragments verify that the deexcitation modifies the results largely.

DOI: 10.1103/PhysRevC.89.057602 PACS number(s): 25.70.Pq, 21.65.Cd, 25.70.Mn

I. Introduction. The isobaric methods have attracted much attention for their possibility to study the nuclear symmetry energy (NSE) of finite nuclei (especially neutron-rich nuclei) and nuclear matter produced in the colliding source of heavy-ion collisions (HICs). For example, the coefficient of symmetry energy ($a_{\rm sym}$) can be obtained via the isobaric binding energy difference [1–3]. In HICs above the Fermi energy, the ratio of $a_{\rm sym}$ to temperature ($a_{\rm sym}/T$) for (neutron-rich) fragments [4–12], the symmetry energy of colliding sources by different scaling techniques [10–12], the difference between chemical potentials of neutrons and protons [13,14], and the temperatures related to the measured fragments [10,15,16] are also studied via isobaric yield ratios. The name "nuclear symmetry energy" is used for nuclear matters ranging from a finite nucleus to dense nuclear matters, which has different values [10–12]. Thus in comparison between the NSE of different nuclear matters, it should be clarified what the nuclear matter is the NSE for [13,14].

An isobaric yield ratio difference (IBD) method is proposed to study the chemical potential difference between neutrons and protons in HICs [13,14]. The isobaric yield ratio (IYR) differing two units in $I = N - Z$ [N (Z) denoting the neutron (proton) numbers] is defined as

$$R(I+2,I,A) = Y(A,I+2)/Y(A,I), \tag{1}$$

in which Y is the yield of the fragment; and A and I are the mass and neutron-excess of the fragment, respectively. From Eq. (1), the IBD between two reactions of similar measurements can be defined, which likes the definition in isoscaling methods [17–19]. In the grand-canonical ensembles theory within the grand canonical limit [20,21], the relationship between the IBD and the ratio of the chemical potential difference between neutrons and protons to temperature ($\Delta\mu_{21}/T$) is written as follows [13,14],

$$\begin{aligned}\Delta\mu_{21}/T &= \ln[R_2(I+2,I,A)] - \ln[R_1(I+2,I,A)] \\ &= (\Delta\mu_{n21} - \Delta\mu_{p21})/T \\ &= [\mu_{n2} - \mu_{n1} - (\mu_{p2} - \mu_{p1})]/T,\end{aligned} \tag{2}$$

in which indices 1 and 2 denote the reaction systems; $\Delta\mu_{n21}/T$ is named as IB-$\Delta\mu_{n21}/T$ since it is obtained from the IBD, i.e., $\ln[R_2(I+2,I,A)] - \ln[R_1(I+2,I,A)]$; T is temperature, which is assumed to be the same in the two reactions; and μ_n (μ_p) is the chemical potential of neutrons (protons), which is determined by neutron (proton) density.

The IB-$\Delta\mu_{21}/T$ is found to indicate the difference between neutron and proton densities of projectiles [13,14]. The neutron density distribution is assumed to vary with the isospin of a calcium isotope, but the variation is hard to be detected experimentally. In this Brief Report, we study the neutron density difference between the calcium isotopes using the IBD method by simulating the reactions induced by them. The modified statistical abrasion-ablation (SAA) model is adopted to calculate the cross sections of prefragments and final fragments in reactions for the IBD analysis.

II. Model Description. The SAA model is a two-stage model to predict fragment yield in HICs [22,23]. By distinguishing the neutron and proton densities, the modified SAA model can well reproduce isotopic (isotonic) yields in asymmetric reactions systems [24–26], and can be used to investigate phenomena originated from neutron-proton asymmetry or neutron skins [26–33]. In the SAA model, the first stage describes the collision in which the nuclei are assumed to be infinitesimal parallel tubes orienting along the beam direction. Independent nucleon-nucleon collisions are taken for the participants in the overlapping zone of the projectile and target nuclei. For an infinitesimal tube inside the projectile, the transmission probabilities for neutrons (protons) at a given impact parameter $\vec{b}$ are given by

$$t_k(\vec{s}-\vec{b}) = \exp\{-[\rho_n^T(\vec{s}-\vec{b})\sigma_{nk} + \rho_p^T(\vec{s}-\vec{b})\sigma_{pk}]\}, \tag{3}$$

*machunwang@126.com

where ρ^T is the nuclear-density distribution of the target nucleus integrated along beam direction, the vectors $\vec{s}$ and $\vec{b}$ are defined in the plane perpendicular to beam, and $\sigma_{k'k}$ is the free space nucleon-nucleon reaction cross section. At a given $\vec{b}$, the average absorbed mass in the infinitesimal tubes is

$$\langle \Delta A(b) \rangle = \int d^2 s \rho_n^T(\vec{s})[1 - t_n(\vec{s} - \vec{b})] + \int d^2 s \rho_p^T(\vec{s})[1 - t_p(\vec{s} - \vec{b})]. \quad (4)$$

The cross section for a prefragment (N, Z) can be calculated from

$$\sigma(\Delta N, \Delta Z) = \int d^2 b P(\Delta N, b) P(\Delta Z, b), \quad (5)$$

where $P(\Delta N, b)$ and $P(\Delta Z, b)$ are the probability distributions for the abraded neutrons and protons at a given b, respectively.

In the second stage, light particles are evaporated from the hot prefragment, which produces measurable final fragments. The evaporation is described by a conventional statistical model under the assumption of thermal equilibrium [23]. The excitation energy of a projectile spectator is estimated by a simple relation of $E^* = 13.3\langle A(b) \rangle$ MeV.

The Fermi-type density distribution for ρ_n (ρ_p) is adopted:

$$\rho_i(r) = \frac{\rho_i^0}{1 + \exp\left(\frac{r - C_i}{t_i/4.4}\right)}, \quad i = n, p, \quad (6)$$

where ρ_i^0 is a normalization constant, r is the radius, t_i is the diffuseness parameter, and C_i is the radius at the half density of the ρ_n (ρ_p) distribution.

III. Results and Discussion. The 80A MeV ^{38,40,42,44,46,48,50,52}Ca + ^{12}C reactions are calculated by using the modified SAA model. In the analysis, the fragments in the ^{40}Ca reaction are labeled as 1, and those in the other reactions as 2. For simplification, the involved reactions in IBD are labeled as ^{X}Ca/^{40}Ca. The IB-$\Delta\mu_{21}/T$ obtained from the prefragments and final fragments are plotted in Fig. 1. In the calculation, the very neutron-rich prefragments do not survive the deexcitation; thus only fragments with I from -1 to 2 are plotted.

First, the IB-$\Delta\mu_{21}/T$ from the prefragments and final fragments have a distribution of one plateau part when the mass of a fragment is small and is the part which increases with A. The distribution is similar to those of the measured fragments studied in Refs. [13,14]. The IB-$\Delta\mu_{21}/T$ from prefragments in the ^{38}Ca/^{40}Ca reactions is reverse to those in the other reactions, which is negative, because that the proton-rich ^{38}Ca reaction is set as reaction 2. The height of IB-$\Delta\mu_{21}/T$ from the prefragments is shown to be sensitive to the isospin of the projectile, which increases as the projectile becomes more neutron rich. It has been noted that μ_n (μ_p) is determined by the nuclear density, and $\Delta\mu_n$ $(\Delta\mu_p)$ reflects the difference between the neutrons (protons) density. The yield of a prefragment is also mainly determined by ρ_n and ρ_p according to Eq. (4). It is illuminating to see the density difference between the projectiles. The averaged IB-$\Delta\mu_{21}/T$ in the plateau part ($\langle \Delta\mu_{21}/T \rangle$) for prefragments is plotted as

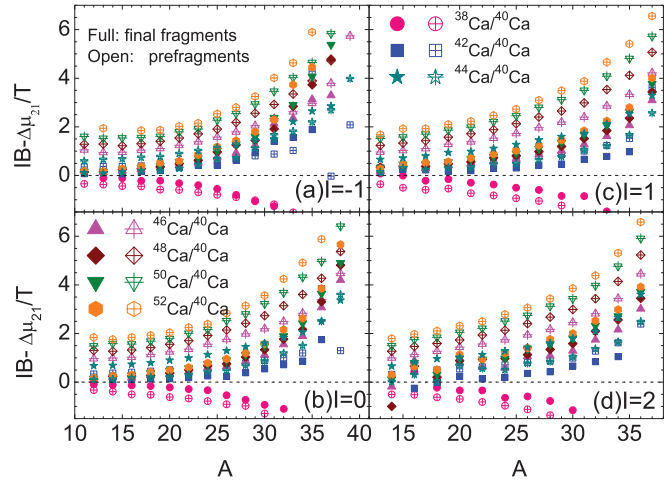

FIG. 1. (Color online) IB-$\Delta\mu_{21}/T$ obtained from the IBD for the prefragments and final fragments between the $^{38,42-52}$Ca/^{40}Ca reactions. The full and open symbols denote the results for the final fragments and prefragments calculated by using the modified SAA model, respectively.

the function of I in Fig. 2. $\langle \Delta\mu_{21}/T \rangle$ shows a regular increase as the projectile becomes more neutron rich. The difference between ρ_n of ^{X}Ca and ^{40}Ca (defined as $\Delta\rho_n$) is plotted in the inset of Fig. 2. $\Delta\rho_n$ is shown first increasing with the radius r, but then decreasing when $r > \sim 2.5$ fm. At the same time, $\Delta\rho_n$ also increase regularly with the asymmetry of the projectile (the trend of $\Delta\rho_n$ between ^{38}Ca/^{40}Ca is inverse to the other projectiles). The similar trend of IB-$\Delta\mu_{21}/T$ (at the same time $\langle \Delta\mu_{21}/T \rangle$) and $\Delta\rho_n$ (when $r < 2.5$ fm) indicates that they have an intrinsic correlation. The very small gap in $\Delta\rho_n$ between the projectiles (about 0.03 fm^{-3}) corresponds to a $\sim$0.3 gap in $\langle \Delta\mu_{21}/T \rangle$, which is enlarged 100 times. The result indicates that IB-$\Delta\mu_{21}/T$ obtained from the prefragment is very sensitive to $\Delta\rho_n$ between the projectiles.

Second, the results in Fig. 1 also show large difference between the IB-$\Delta\mu_{21}/T$ determined from the final fragments and the prefragments. As the projectile becomes more neutron

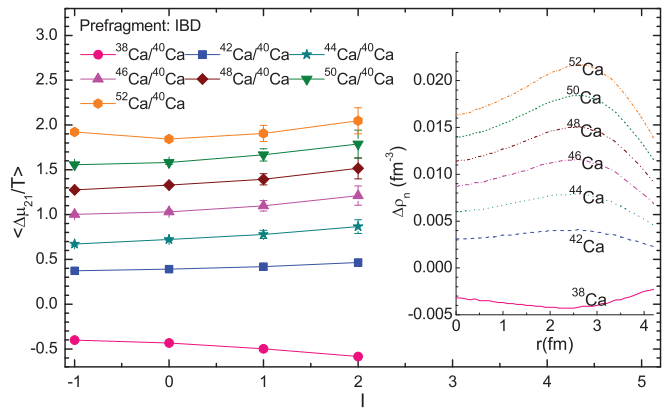

FIG. 2. (Color online) The averaged IB-$\Delta\mu_{21}/T$ ($\langle \Delta\mu_{21}/T \rangle$) of the plateau part for prefragments plotted in Fig. 1. The inset shows the difference between the neutron density distributions of ^{X}Ca and ^{40}Ca [$\Delta\rho_n = \rho_n(^{X}\text{Ca}) - \rho_n(^{40}\text{Ca})$].

rich, the obvious regular increasing of IB-$\Delta\mu_{21}/T$ from the prefragments vanishes in the results from the final fragment, especially when the fragment has a small mass. The height of the plateau part in the IB-$\Delta\mu_{21}/T$ from the final fragment also becomes very similar. The large difference between the IB-$\Delta\mu_{21}/T$ from the prefragments and the final fragments clearly shows that the results are largely modified by the evaporation process. Relatively high plateaus are found in $\Delta\mu_{21}/T$ from the measured fragments [13,14], while the SAA results are much lower than the measured fragments, and the SAA IB-$\Delta\mu_{21}/T$ from the final fragments is less sensitive to the asymmetry of the projectile. The comparison between the IB-$\Delta\mu_{21}/T$ from the SAA prefragments and final fragments only verifies that the evaporation process largely modifies the results of the observable which is constructed from the fragment yield in experiments and theories, such as the isobaric yield ratio [5,11,12,33], the ratio of symmetry-energy coefficient to temperature [8–10], isoscaling [34], etc.

At last, to see why the IB-$\Delta\mu_{21}/T$ obtained from the final fragments are similar in the calculated reactions but differ largely from the measured ones, the yields of the calculated final fragments and the measured data in the ^{40,48}Ca + ^{9}Be reactions [35] are compared in Fig. 3. It should be noted that, though the measured yield of a fragment is from the reactions at an incident energy of 140A MeV, the SAA results are similar since the incident energy only changes the nucleus-nucleus cross section [36]. As illustrated in Fig. 3, for most fragments in the ^{40}Ca + ^{9}Be reaction, in each I chain, the SAA result can well predict the measured cross sections except for the odd-even staggering phenomena. While for fragments in the ^{48}Ca + ^{9}Be reaction, the yields deviate from the measured results largely in the $I = -1$, 0, and 1 isobaric chains. Compared to the large gaps between the measured yields of fragments in the $I = -1$, 0, and 1 isobaric chains, the

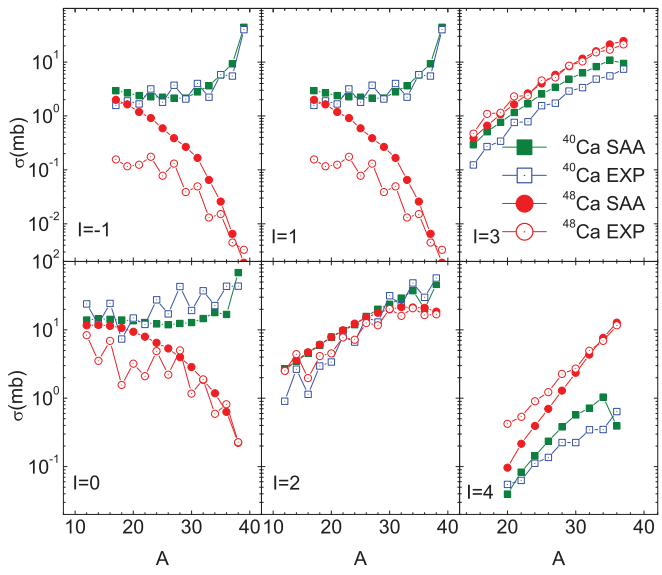

FIG. 3. (Color online) Cross sections of the SAA final fragments and the measured ones in the ^{40,48}Ca + ^{9}Be reactions (the measured reactions are at 140A MeV [35]). The full and open symbols denote the SAA and experimental results, respectively.

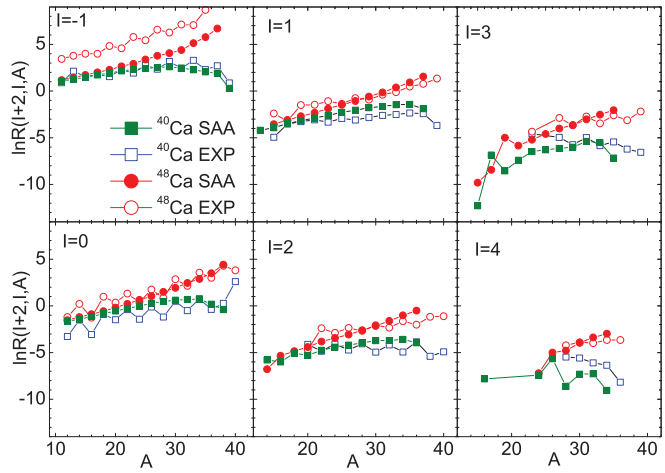

FIG. 4. (Color online) Comparison between the IYRs from final fragments in the SAA calculated and the measured ones in the ^{40,48}Ca + ^{9}Be reactions, which are denoted by the full and open symbols, respectively.

difference between the calculated yields of fragments are much smaller. The relatively small difference between ρ_n of ^{48}Ca and ^{40}Ca, which is calculated according to Eq. (6), results in the overestimation of the $I = -1$, 0, and 1 fragments. This also can account for the underestimation of the IYR for mirror nuclei in reactions [33].

In Fig. 4, the IYRs for the SAA final fragments and the measured ones are plotted. The IYRs for the SAA final fragments well reproduce the experimental ones except that for the mirror nuclei in the ^{48}Ca reactions. Though the IYRs for the SAA results are close to the measured ones, the similar IYRs for the calculated small mass fragments makes it unable to reproduce the gaps between IYRs in the measured ^{48}Ca/^{40}Ca reactions. Especially, for the mirror fragments, the SAA IYR is much smaller than the experimental one. Combining the comparison between the SAA and experimental yields of final fragments, and the resultant IYRs, it is the relatively small $\Delta\rho_n$ between projectiles according to the Fermi-type density distribution that makes the IB-$\Delta\mu_{21}/T$ from the final fragments insensitive to the density difference.

IV. Summary. In summary, the probe IB-$\Delta\mu_{21}/T$, which denotes the difference between the chemical potentials of neutrons and protons, is used to study the neutron density difference between ^{40}Ca and its isotopes. The modified SAA model is adopted to calculate yields of prefragments and final fragments in the calcium isotopes induced reactions. The height of IB-$\Delta\mu_{21}/T$ from the prefragments are found to be sensitive to the difference between the neutron density distributions of calcium isotopes, especially when the fragment has a small mass. But the sensitivity of the IB-$\Delta\mu_{21}/T$ from prefragments becomes much lower in the calculated final fragments, which is different from the measured results. The phenomena are interpreted as the slight change of $\Delta\rho_n$ according to the Fermi-type density distribution. The large difference between the IB-$\Delta\mu_{21}/T$ obtained from prefragments and final fragments shows that the deexcitation process largely modifies the results of probes based on fragment yields.

This work is supported by the National Natural Science Foundation of China under Grant No. 10905017, the Program for Science & Technology Innovation Talents in Universities of Henan Province (Grant No. 13HASTIT046), and the Young Teacher Project in Henan Normal University (HNU), China.

[1] J. Jänecke and T. W. O'Donnell, Nucl. Phys. A **781**, 317 (2007).
[2] H. Mei, Y. Huang, J. M. Yao, and H. Chen, J. Phys. G: Nucl. Part. Phys. **39**, 015107 (2012).
[3] C. W. Ma *et al.*, Chin. Phys. Lett. **29**, 092101 (2012).
[4] M. Huang, A. Bonasera, Z. Chen, R. Wada, K. Hagel, J. B. Natowitz, P. K. Sahu, L. Qin, T. Keutgen, S. Kowalski, T. Materna, J. Wang, M. Barbui, C. Bottosso, and M. R. D. Rodrigues, Phys. Rev. C **81**, 044618 (2010).
[5] M. Huang *et al.*, Phys. Rev. C **81**, 044620 (2010).
[6] P. Marini *et al.*, Phys. Rev. C **85**, 034617 (2012).
[7] C.-W. Ma, F. Wang, Y.-G. Ma, and C. Jin, Phys. Rev. C **83**, 064620 (2011).
[8] C.-W. Ma *et al.*, Eur. Phys. J. A **48**, 78 (2012).
[9] C.-W. Ma *et al.*, Chin. Phys. Lett. **29**, 062101 (2012); Chin. Phys. C **37**, 024101 (2013).
[10] C.-W. Ma *et al.*, Chin. Phys. C **37**, 024102 (2013).
[11] S. Mallik and G. Chaudhuri, Phys. Rev. C **87**, 011602(R) (2013).
[12] P. Marini *et al.*, Phys. Rev. C **87**, 024603 (2013).
[13] C.-W. Ma, S.-S. Wang, Y.-L. Zhang, and H.-L. Wei, Phys. Rev. C **87**, 034618 (2013).
[14] C.-W. Ma, S.-S. Wang, Y.-L. Zhang, and H.-L. Wei, J. Phys. G: Nucl. Part. Phys. **40**, 125106 (2013).
[15] C. W. Ma, J. Pu, Y. G. Ma, R. Wada, and S. S. Wang, Phys. Rev. C **86**, 054611 (2012).
[16] C.-W. Ma *et al.*, Phys. Rev. C **88**, 014609 (2013).
[17] H. S. Xu *et al.*, Phys. Rev. Lett. **85**, 716 (2000).
[18] Y. G. Ma *et al.*, Phys. Rev. C **69**, 064610 (2004); **72**, 064603 (2005).
[19] M. B. Tsang *et al.*, Phys. Rev. Lett. **86**, 5023 (2001).
[20] C. B. Das, S. Das Gupta, X. D. Liu, and M. B. Tsang, Phys. Rev. C **64**, 044608 (2001).
[21] M. B. Tsang *et al.*, Phys. Rev. C **76**, 041302(R) (2007).
[22] T. Brohm and K.-H. Schmidt, Nucl. Phys. A **569**, 821 (1994).
[23] J. J. Gaimard and K. H. Schmidt, Nucl. Phys. A **531**, 709 (1991).
[24] H.-L. Wei and C.-W. Ma, Acta Phys. Sin. **59**, 5364 (2010) (in Chinese).
[25] C.-W. Ma *et al.*, Phys. Rev. C **79**, 034606 (2009).
[26] D. Q. Fang *et al.*, Phys. Rev. C **61**, 044610 (2000).
[27] D. Q. Fang *et al.*, J. Phys. G: Nucl. Part. Phys. **34**, 2173 (2007).
[28] C.-W. Ma, H.-L. Wei, G.-J. Liu, and J.-Y. Wang, J. Phys. G: Nucl. Part. Phys. **37**, 015104 (2010).
[29] D. Q. Fang, Y. G. Ma, X. Z. Cai, W. D. Tian, and H. W. Wang, Phys. Rev. C **81**, 047603 (2010).
[30] C.-W. Ma, H.-L. Wei, and M. Yu, Phys. Rev. C **82**, 057602 (2010).
[31] C.-W. Ma *et al.*, Chin. Phys. B **17**, 1216 (2008).
[32] C.-W. Ma and S.-S. Wang, Chin. Phys. C **35**, 1017 (2011).
[33] C.-W. Ma, S.-S. Wang, H.-L. Wei, and Y.-G. Ma, Chin. Phys. Lett. **30**, 052501 (2013); C.-W. Ma, H.-L. Wei, and Y.-G. Ma, Phys. Rev. C **88**, 044612 (2013).
[34] P. Zhou *et al.*, Phys. Rev. C **84**, 037605 (2011).
[35] M. Mocko *et al.*, Phys. Rev. C **74**, 054612 (2006).
[36] Cai Xiangzhou, Feng Jun, Shen Wenqing, Ma Yugang, Wang Jiansong, and Ye Wei, Phys. Rev. C **58**, 572 (1998).